

Video Based Face Recognition Using Graph Matching

Gayathri Mahalingam and Chandra Kambhamettu

Video/Image Modeling and Synthesis (VIMS) Laboratory,
Department of Computer and Information Sciences, University of Delaware, Newark,
DE, USA

Abstract. In this paper, we propose a novel graph based approach for still-to-video based face recognition, in which the temporal and spatial information of the face from each frame of the video is utilized. The spatial information is incorporated using a graph based face representation. The graphs contain information on the appearance and geometry of facial feature points and are labeled using the feature descriptors of the feature points. The temporal information is captured using an adaptive probabilistic appearance model. The recognition is performed in two stages where in the first stage a Maximum a Posteriori solution based on PCA is computed to prune the search space and select fewer candidates. A simple deterministic algorithm which exploits the topology of the graph is used for matching in the second stage. The experimental results on the UTD database and our dataset show that the adaptive matching and the graph based representation provides robust performance in recognition.

1 Introduction

Face recognition has long been an active area of research, and numerous algorithms have been proposed over the years. For more than a decade, active research work has been done on face recognition from still images or from videos of a scene [1]. A detailed survey of existing algorithms on video-based face recognition can be found in [2] and [3]. The face recognition algorithms developed during the past decades can be classified into two categories: holistic approaches and local feature based approaches. The major holistic approaches that were developed are Principal Component Analysis (PCA) [4], combined Principal Component Analysis and Linear Discriminant Analysis (PCA+LDA) [5], and Bayesian Intra-personal/Extra-personal Classifier (BIC) [6].

Chellappa *et al.* [7] proposed an approach in which a Bayesian classifier is used for capturing the temporal information from a video sequence and the posterior distribution is computed using sequential importance sampling. As for the local feature based approaches, Manjunath and Chellappa [8] proposed a feature based approach in which features are derived from the intensity data without assuming any knowledge of the face structure. Topological graphs are used to represent relations between features, and the faces are recognized by matching the graphs. Ersi and Zelek [9] proposed a feature based approach where in a statistical Local

40 Feature Analysis (LFA) method is used to extract the feature points from a face
 41 image. Gabor histograms are generated using the feature points and are used to
 42 identify the face images by comparing the Gabor histograms using a similarity
 43 metric. Wiskott *et al.* [10] proposed a feature based graph representation of the
 44 face images for face recognition in still images. The face is represented as a graph
 45 with the features as the nodes and each feature described using a Gabor jet. The
 46 recognition is performed by matching graphs and finding the most similar ones.
 47 A similar framework was proposed by Ersi *et al.* [11] in which the graphs were
 48 generated by triangulating the feature points.

49 Most of these approaches focused on image-based face recognition applica-
 50 tions. Various approaches to video-based face recognition have been studied in
 51 the past, in which both the training and test set are video sequences. Video-based
 52 face recognition has the advantage of using the temporal information from each
 53 frame of the video sequence. Zhou *et al.* [12] proposed a probabilistic approach
 54 in which the face motion is modeled as a joint distribution, whose marginal
 55 distribution is estimated and used for recognition. Li [13] used the temporal in-
 56 formation to model the face from the video sequence as a surface in a subspace
 57 and performed recognition by matching the surfaces. Kim *et al.* [14] recognized
 58 faces from video sequences by fusing pose-discriminant and person-discriminant
 59 features by modeling a Hidden Markov Model (HMM) over the duration of a
 60 video sequence. Stallkamp *et al.* [15] proposed a classification sub-system of
 61 a real-time video-based face identification system. The system uses K-nearest
 62 neighbor model and Gaussian mixture model (GMM) for classification purposes
 63 and uses distance-to-model, and distance-to-second-closest metrics to weight the
 64 contribution of each individual frame to the overall classification decision.

65 Liu and Chen [16] proposed an adaptive HMM to model the face images
 66 in which the HMM is updated with the result of identification from the pre-
 67 vious frame. Lee *et al.* [17] represented each individual by a low-dimensional
 68 appearance manifold in the ambient image space. The model is trained from a
 69 set of video sequences to extract a transition probability between various poses
 70 and across partial occlusions. Park and Jain [18] proposed a 3D model based ap-
 71 proach in which a 3D model of the face is used to estimate the pose of the face in
 72 each frame and then matching is performed by extracting the frontal pose from
 73 the 3D model. Xu *et al.* [19] proposed a video based face recognition system in
 74 which they integrate the effects of pose and structure of the face and the illumi-
 75 nation conditions for each frame in a video sequence in the presence of multiple
 76 point and extended light sources. The pose and illumination estimates in the
 77 probe and gallery sequences are then compared for recognition applications.

78 In this paper, we propose a novel graph based approach for image-to-video
 79 based face recognition which utilizes the spatial and temporal characteristics
 80 of the face from the videos. The face is spatially represented by constructing
 81 a graph using the facial feature points as vertices and labeling them with their
 82 feature descriptors. A probabilistic mixture model is constructed for each subject
 83 which captures the temporal information. The recognition is performed in two
 84 stages where in the first stage the probabilistic mixture model is used to prune

85 the search space using a MAP rule. A simple deterministic algorithm that uses
 86 cosine similarity measure is used to compare the graphs in the second stage.
 87 The probabilistic models are updated with the results of recognition from each
 88 frame of the video sequence, thus making them adaptive. Section 2 explains
 89 our procedure in constructing the graphs and the adaptive probabilistic mixture
 90 models for each subject. The two stage recognition is explained in section 5.

91 2 Face Image Representation

92 In this section, we describe our approach in extracting the facial feature points
 93 and their descriptors which are used in the spatial representation of the face
 94 images. Every face is distinguished not by the properties of individual features,
 95 but by the contextual relative location and comparative appearance of these
 96 features. Hence it is important to identify those features that are conceptually
 97 common in every face such as eye corners, nose, mouth, etc. In our approach,
 98 the facial feature points are extracted using a modified Local Feature Analysis
 99 (LFA) technique, and extracted feature points are described using Local Binary
 100 Pattern (LBP) [20], [21] feature descriptors.

101 2.1 Feature Point Extraction

102 The Local Feature Analysis (LFA) proposed by Penev and Atick [22] constructs
 103 kernels, which are basis vectors for feature extraction. The kernels are con-
 104 structed using the eigenvectors of the covariance matrix of the vectorized face
 105 images. LFA is referred to as a local method since it constructs a set of kernels
 106 that detects local structure; e.g., nose, eye, jaw-line, and cheekbone, etc. The
 107 local kernels are optimally matched to the second-order statistics of the input
 108 ensemble [22]. Given a set of n d -dimensional images x_1, \dots, x_n , Penev and
 109 Atick [22] compute the covariance matrix C , from the zero-mean matrix X of
 110 the n vectorized images as follows:

$$C = XX^T. \quad (1)$$

111 The eigenvalues of the covariance matrix C are computed and the first k largest
 112 eigenvalues, $\lambda_1, \lambda_2, \dots, \lambda_k$, and their associated eigenvectors ψ_1, \dots, ψ_k to
 113 define the kernel K ,

$$K = \Psi \Lambda \Psi^T \quad (2)$$

114 where $\Psi = [\psi_1 \dots \psi_k]$, $\Lambda = \text{diag}(\frac{1}{\sqrt{\lambda_r}})$.

115 The rows of K contain the kernels. These kernels have spatially local prop-
 116 erties and are "topographic" in the sense that the kernels are indexed by spatial
 117 location of the pixels in the image, *i.e.*, each pixel in the image is represented by
 118 a kernel from K . Figure 1(a) shows the kernels corresponding to the nose, eye,
 119 mouth and cheek positions. The kernel matrix K transforms the input image
 120 matrix X to the LFA output $O = K^T X$ which inherits the same topography as
 121 the input space.

122 Hence, the dimension of the output is reduced by choosing a subset of kernels,
 123 M , where M is a subset of indices of elements of K . These subsets of kernels
 124 are considered to be at those spatial locations which are the feature points of
 125 the face image. Penev and Atick [22] proposed an iterative algorithm that uses
 126 the mean reconstruction error to construct M by adding a kernel at each step
 127 whose output produces the maximum reconstruction error,

$$\arg \max_x (\|O(x) - O^{rec}(x)\|^2) \quad (3)$$

128 where $O^{rec}(x)$ is the reconstruction of the output $O(x)$.

129 Although mean reconstruction error is a useful criterion for representing data,
 130 it does not guarantee an effective discrimination between data from different
 131 classes as the kernels selection process aims at reducing the reconstruction error
 132 for the entire image and not the face region. Hence, we propose to use the Fisher's
 133 linear discriminant method [23] to select the kernels that characterize the most
 134 discriminant and descriptive feature points of different classes. We compute the
 135 Fisher scores using the LFA output O . Fisher score is a measure of discriminant
 136 power which estimates how well different classes of data are separated from each
 137 other, and is measured as the ratio of variance between the classes to the variance
 138 within the classes. Given the LFA output $O = [o_1 \dots o_n]$ for c classes, with each
 139 class having n_i samples in the subset χ_i , the Fisher score of the x^{th} kernel, $J(x)$
 140 is given by

$$J(x) = \frac{\sum_{i=1}^c n_i (m_i(x) - m(x))^2}{\sum_{i=1}^c \sum_{o \in \chi_i} (o(x) - m_i(x))^2} \quad (4)$$

141 where $m(x) = \frac{1}{n} \sum_{i=1}^c n_i m_i(x)$ and $m_i(x) = \frac{1}{n_i} \sum_{o \in \chi_i} o(x)$. The kernels that
 142 correspond to high Fisher scores are chosen to represent the most discriminative
 143 feature points of the image. Figure 1(b) shows the set of feature points extracted
 144 using the Fisher scores.



(a) $K(x, y)$ derived from a set of 315 images (b) The first 100 feature points extracted from the training images

Fig. 1. 1(a) shows $K(x, y)$ at the nose, mouth, eye, and cheeks and 1(b) shows the feature points extracted (best viewed in color).

145 2.2 Feature Description with Local Binary Pattern

146 A feature descriptor is constructed for each feature point extracted from an
 147 image using Local Binary Pattern (LBP).

148 The original Local Binary Pattern (LBP) operator proposed by Ojala *et al.*
 149 [20] is a simple but very efficient and powerful operator for texture description.
 150 The operator labels the pixels of an image by thresholding the $n \times n$ neighborhood
 151 of each pixel with the value of the center pixel, and considering the result value
 152 as a binary number. Figure 2(a) shows an example of the basic LBP operator and
 153 figure 2(b) shows a (4, 1) and (8, 2) circular LBP operator. The histogram of the
 154 labels of the pixels of the image can be used as a texture descriptor. The grey-
 155 scale invariance is achieved by considering a local neighborhood for each pixel,
 156 and invariance with respect to scaling of the grey scale is achieved by considering
 157 just the signs of the differences in the pixel values instead of their exact values.
 158 The LBP operator with P sampling points on a circular neighborhood of radius
 159 R is given by,

$$LBP_{P,R} = \sum_{p=0}^{P-1} s(g_p - g_c) 2^p \quad (5)$$

160 where

$$s(x) = \begin{cases} 1 & \text{if } x \geq 0 \\ 0 & \text{if } x < 0 \end{cases} \quad (6)$$

161 Ojala *et al.* [21] also introduced another extension to the original operator
 162 which uses the property called *uniform patterns* according to which a LBP is
 163 called uniform if there exist at most two bitwise transitions from 0 to 1 or vice
 164 versa. Uniform patterns can reduce the dimension of the LBP significantly which
 165 is advantageous for face recognition.

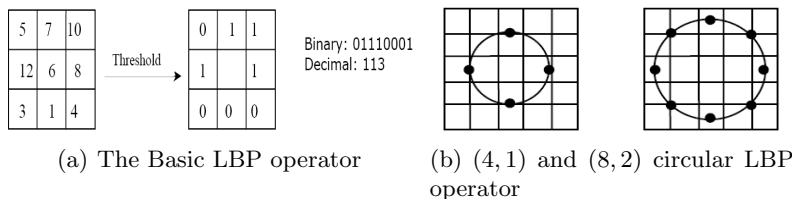


Fig. 2. The basic LBP operator and the circular LBP operator

166 In our experiments, we use $LBP_{8,2}^u$ operator which denotes a uniform LBP
 167 operator with 8 sampling pixels in a local neighborhood region of radius 2. A
 168 5×5 window around the pixel is chosen as the neighborhood region and a feature
 169 vector of length 59 is obtained.

170 3 Image Graph Construction

171 The most distinctive property of a graph is its geometry, which is determined by
 172 the way the vertices of the graph are arranged spatially. Graph geometry plays

173 an important role in discriminating the graphs of different face images. In our
 174 approach, the graph geometry is defined by constructing a graph with constraints
 175 imposed on the length of the edges between a vertex and its neighbors.

176 Considering that we extract around n feature points from each face image,
 177 at least $n!$ graphs can be generated for each image. Evaluating this number of
 178 graphs for each probe image would be very computationally expensive. Hence,
 179 a graph generating procedure that generates a unique graph with the given set
 180 of vertices is proposed. At each iteration, vertices and edges are added to the
 181 graph in a Breadth-first search manner and considering a spatial neighborhood
 182 distance for each vertex. This generates a unique graph for a set of feature points.
 183 The procedure to generate a graph given a set of vertices is given as follows;

```

184 1 Pick a random vertex  $v$  from the list of vertices of the graph.
185 2 Add  $v$  to the end of the queue  $q$ .
186 3 While NOT all the vertices have been visited
187     Pick a vertex  $u$  from the front of the queue  $q$ .
188     If  $u$  is not visited
189         Find the Neighbors  $N$  of  $u$  who are within a Euclidean distance.
190         Add  $N$  to the queue  $q$ .
191         Mark  $u$  as visited
192     endif
193 endwhile

```

194 The idea behind representing face images using graphs is mainly due to the
 195 spatial properties of the graph, as a graph can represent the inherent shape
 196 changes of a face and also provide a simple, but powerful matching technique to
 197 compare graphs.

198 4 Probabilistic Graph Appearance Model

199 The appearance of a graph is another important distinctive property and is de-
 200 scribed using the feature descriptors of the vertices of the graph. An efficient as
 201 well as effective description of the appearance of the vertices of the graphs is re-
 202 quired in order construct a graph appearance model that elevates the distinctive
 203 properties of the face of an individual. Modeling the joint probability distribu-
 204 tion of the appearance of the vertices of the graphs of an individual produces an
 205 effective representation of the appearance model through a probabilistic frame-
 206 work. Since the model is constructed using the feature descriptors, it is easy to
 207 adapt the model to the changes in the size of the training data for the individ-
 208 ual. Given N individuals and M training face images, the algorithm to learn the
 209 model is described as follows:

```

210 1. Initialize  $N$  model sets.
211 2. For each training image  $I_c^j$ , ( $j^{th}$  image of the  $c^{th}$  individual)
212     a. Extract the feature points (as described in Subsection 2.1).

```

- 213 b. Compute feature descriptors for each feature point (as described in Sub-
 214 section 2.2).
 215 c. Construct Image graphs (as described in Subsection 3).
 216 d. Include the graph in the model of the c^{th} individual.
 217 3. Construct the appearance model for each individual using their model sets.

218 In our approach, a probabilistic graph appearance model is generated for
 219 each subject and is used for training purposes. Given a graph $G(V, E)$, where
 220 V is the list of vertices in the graph, and E the set of edges in the graph, the
 221 probability of G belonging to a model set (subject) k is given by,

$$R_k = \max_n P(G|\Phi_n) \quad (7)$$

222 where $P(G|\Phi_n)$ is the posterior probability, and Φ_n is the appearance model for
 223 the n^{th} subject constructed using the set of feature descriptors F of the set of
 224 vertices of all the graphs of the subject. The appearance model Φ_n is constructed
 225 by estimating the joint probability distribution of the appearance of the graphs
 226 for each subject. R_k is called the Maximum a Posteriori (MAP) solution. In our
 227 approach, we estimate the joint probability distribution of the graph appearance
 228 model for each subject using the Gaussian Mixture Model (GMM) [24] which
 229 can efficiently represent heterogeneous data, the dominant patterns which are
 230 captured by the Gaussian component distributions.

231 Given a training face database containing images of L subjects and each
 232 subject having at least one image in the training database, the set of feature
 233 descriptors X for each subject to be used to model the joint likelihood of the
 234 subject will be a $(m \times f) \times t$ distribution, where m is the number of images for
 235 each subject, f is the number of feature points extracted for each image and t
 236 the dimension of the feature vector (in our case, it is 59 and is reduced to 20).
 237 To make the appearance model estimation more accurate and tractable, we use
 238 the Principal Component Analysis (PCA) to reduce the dimensionality of the
 239 feature vectors.

240 Each subject in the database is modeled as a GMM with K Gaussian com-
 241 ponents. The set of feature descriptors X of each subject is used to model the
 242 GMM of that individual. Mathematically, a GMM is defined as:

$$P(X|\theta) = \sum_{i=1}^K w_i \cdot N(X|\mu_i, \sigma_i). \quad (8)$$

243 where

$$244 \quad N(X|\mu_i, \sigma_i) = \frac{1}{\sigma_i \sqrt{2\pi}} \cdot e^{-\frac{(X-\mu_i)^2}{2\sigma_i^2}}$$

245 are the components of the mixture, $\theta = \{w_i, \mu_i, \sigma_i^2\}_{i=1}^K$ includes the parameters
 246 of the model, which includes the weights w_i , the means μ_i , and the variances σ_i^2
 247 of the K Gaussian components.

248 In order to maximize the likelihood function $P(X|\theta)$, the model parameters
 249 are re-estimated using the Expectation-Maximization (EM) technique [25]. The

250 EM algorithm is an iterative procedure to compute the Maximum Likelihood
 251 (ML) estimate in the presence of missing or hidden data. In ML estimation, we
 252 wish to estimate the model parameters for which the observed data are the most
 253 likely:

$$\theta^c = \arg \max_{\theta} P(X|\theta). \quad (9)$$

254 At each iteration of the EM algorithm the missing data are estimated with
 255 the current estimate of the model parameters, and the likelihood function is
 256 maximized with assumption that the missing data are known. For more details
 257 about the EM algorithm see [25].

258 5 Adaptive Matching and Recognition

259 In this section, we describe our two stage matching procedure to adaptively
 260 match every frame of the video sequence and the trained appearance models
 261 and the graphs. In the first stage of the matching process, a MAP solution is
 262 computed for the test graph using the trained appearance models. The MAP
 263 solution is used to prune the search space for the second stage of matching. A
 264 subset of individuals' appearance model and their trained graphs are selected
 265 based on the MAP solution. This subset of appearance models are used in the
 266 second stage of matching process. In the second stage, a simple deterministic
 267 algorithm that uses the cosine similarity measure and the nearest neighborhood
 268 classifier to find the geometrical similarity of the graphs is proposed. The GMM
 269 is adapted with the result of recognition from each frame of the test video se-
 270 quence. We use the likelihood score and the graph similarity score to decide
 271 on the correctness of the recognition and update the appropriate GMM. The
 272 recognition result of a frame is considered correct if the difference between the
 273 highest likelihood score and the second highest likelihood score is greater than
 274 a threshold. A similar difference in graph similarity scores is also computed to
 275 support the decision. This measure of correctness is based on the same idea as
 276 Lowe [26], that reliable matching requires the best match to be significantly bet-
 277 ter than the second-best match. For a given test sequence, the difference in the
 278 likelihood scores and the difference in the similarity scores are computed and the
 279 GMM is updated if these values are greater than a threshold. Given an existing
 280 GMM Θ_{old} and observation vectors O from the test sequence, the new GMM
 281 is estimated using the EM algorithm with Θ_{old} as the initial values. The entire
 282 matching procedure is given as follows;

- 283 1. For *each frame f in the video sequence*
 - 284 a. Extract the facial feature points and their descriptors from f .
 - 285 b. Reduce the dimension of feature descriptors using the projection matrix
 286 from training stage.
 - 287 c. Construct the image graph G .
 - 288 d. Obtain the probability of G belonging to each appearance model, and
 289 select the k model sets with highest probability. k is 10% in our experi-
 290 ments.

- 291 e. Obtain the similarity scores between G and the graphs of k individuals.
 292 f. Update the appropriate appearance model based on the likelihood score
 293 and similarity score.
 294 2. Select the individual with the maximum number of votes from all the frames.

295 The algorithm to find the spatial similarity between two graphs is given as
 296 follows;

- 297 1. For each vertex v in the test graph with a spatial neighborhood W , a search
 298 is conducted over W (in the trained graph) and the best matching feature
 299 vertex u is selected, such that

$$S_{vu} = \frac{f_v \cdot f_u}{|f_v| |f_u|} \quad (10)$$

300 where f_v and f_u are the feature vectors of v and u respectively, and S_{vu} is
 301 the similarity score between v and u .

- 302 2. Repeat step 1 with neighbors of v and so on until all the vertices have been
 303 matched. The sum of the similarity scores of all the vertices gives the measure
 304 of similarity between the two graphs.

305 6 Experiments

306 In order to validate the robustness of the proposed technique, we used a set
 307 of close range and moderate range videos from the UTD database [27]. The
 308 database included 315 subjects with high resolution images in various poses.
 309 The videos included subjects with neutral expression and also walking towards
 310 the camera from a distance. We also generated a set of moderate range videos
 311 (both indoor and outdoor) with 6 subjects. Figure 3 shows sample video frames
 312 from the UTD dataset and figure 4 shows sample video frames from our dataset.

313 In the preprocessing step, the face region is extracted from the image, nor-
 314 malized using histogram equalization technique and are resized to 72×60 pixels.
 315 150 features were extracted and a LBP is computed for each feature point. PCA
 316 is performed on the feature vectors to reduce the dimension from 59 to 20 (with
 317 nearly 80% of the non-zero eigenvalues retained). A graph is generated for each
 318 face image with a maximum spatial neighborhood distance of 30 pixels. A graph
 319 space model is constructed for each subject using GMM with 10 Gaussian com-
 320 ponents.

321 During the testing stage, in order to mimic the practical situation, we con-
 322 sider a subset of frames in which an individual appear in the video and use it
 323 for testing purposes. We randomly select an individual and a set of frames that
 324 include the individual. The preprocessing and the graph generation procedure
 325 similar to those performed in the training stage are applied to each frame of
 326 the video sequence. The likelihood scores are computed for the test graph and
 327 the GMMs and the training graphs are matched with the test graph to produce
 328 similarity scores, and the appropriate GMM is updated using the similarity and



(a) Sample frames from close-range videos of UTD dataset



(b) Sample frames from moderate-range videos of UTD dataset

Fig. 3. Sample video frames from the UTD video dataset

329 likelihood scores. The threshold is determined by the average of the difference
 330 in likelihood scores and similarity scores between each class of data. Though the
 331 threshold value is data dependent, the average proves to be an optimum value.

Table 1. Comparison of the error rates with different algorithms

	HMM	AGMM	Graphs	AGMM+Graphs
UTD Database (close-range)	24.3%	24.1%	23.2%	20.1%
UTD Database (moderate-range)	31.2%	31.2%	29.8%	25.4%
Our Dataset	8.2%	3.4%	2.1%	1.1%

332 The performance of the algorithm is compared with video-based recognition
 333 algorithm in [16] which handles video-to-video based recognition. The algorithm
 334 in [16] performs eigen analysis on the face images and uses an adaptive Hid-
 335 den Markov Model (HMM) for recognition. We also test the performance of the
 336 system with only the adaptive graph appearance model (AGMM) and the ap-
 337 pearance model with the graph model sets (AGMM+Graphs). The results are
 338 tabulated in the Table 1. Figure 5 shows the Cumulative Match Characteristic
 339 curve obtained for various algorithms (HMM, AGMM and AGMM+Graphs) on
 340 the UTD dataset.

341 From the error rates we can see that the performance of our approach is
 342 definitely promising when compared with the other approaches. The account
 343 of spatial and temporal information together improves the performance of the
 344 recognition process. The number of images in the training dataset played an
 345 important role in the performance, as it is evident from the error rates. The close-
 346 range videos of the UTD database has lower error rates than the moderate-range
 347 videos. This is due to the reason that the frame of the video sequence mostly
 348 contains the face region thus gathering more details of the facial features than

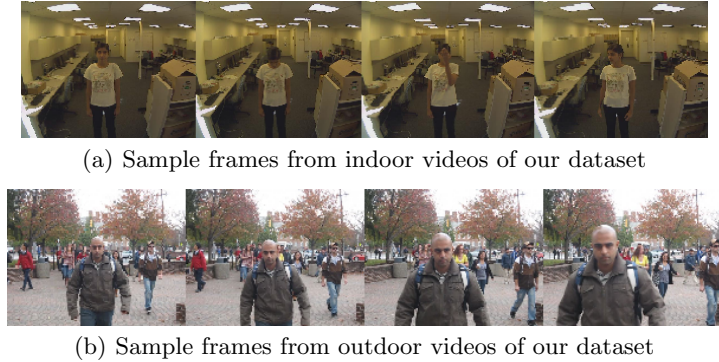


Fig. 4. Sample video frames from our video dataset

349 the moderate-range videos. The number of training set images for each subject
 350 played a role in the performance. The UTD dataset included 3 training images
 351 for each subject whereas our dataset included at least 5 training images. The
 352 algorithm shows a high recognition rate when experimented on our dataset as it
 353 can be seen for the error rates. Though there were limited number of subjects in
 354 the dataset, the videos in the dataset included both indoor and outdoor videos
 355 taken using a PTZ camera which is mainly used for surveillance. The system
 356 provided a better performance with both indoor and outdoor videos which has
 357 different illumination, pose changes and in moderate range.

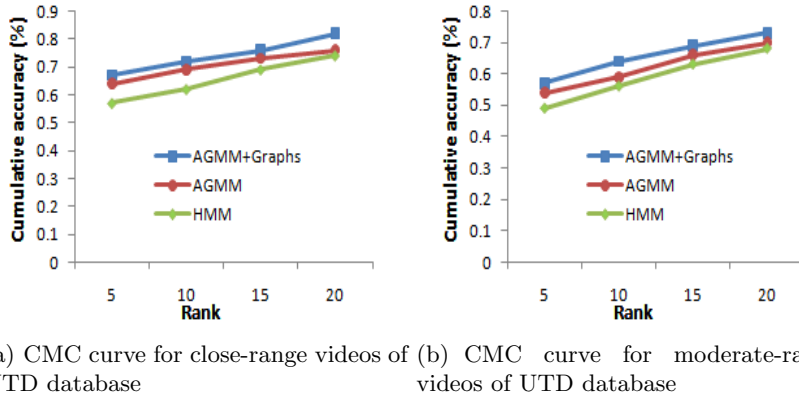


Fig. 5. Cumulative Match Characteristic curves for close-range and moderate-range videos

358 The system performs better as a video based face recognition system than
 359 a still image based face recognition system, due to the wealth of temporal in-
 360 formation available from the video sequence and the effective use of it by the

361 proposed adaptive probabilistic model. As a still image based face recognition,
 362 an image with a frontal pose of the face yields better performance than non
 363 frontal pose image. Thus, pose of the face image plays a role in the recognition.
 364 Also, the system's performance is affected by the comparison of a single high res-
 365 olution image with a low resolution frame in a still image based face recognition
 366 system. Thus the adaptive matching technique combined with the graph based
 367 representation is significantly an advantage in matching images with videos.

368 From our experiments, we found that changing the value of the parameters
 369 did not significantly change the performance of the system and the values that we
 370 used tend to be the optimum. For example, increasing the maximum Euclidean
 371 distance between two vertices of a graph to a value greater than the width or
 372 length of the image will have no effect as the graph will always be connected as
 373 the distance between two vertices will never be greater than these values.

374 7 Conclusion

375 In this paper, we proposed a novel technique for face recognition from videos.
 376 The proposed technique utilizes both the temporal and spatial characteristics of
 377 a face image from the video sequence. The temporal characteristics are captured
 378 by constructing a probabilistic appearance model and a graph is constructed
 379 for each face image using the set of feature points as vertices of the graph and
 380 labeling it with the feature descriptors. A modified LFA and LBP were used to
 381 extract the feature points and feature descriptors respectively. The appearance
 382 model is built using GMM for each individual in the training stage and is adapted
 383 with the recognition results of each frame in the testing stage. A two stage
 384 matching procedure that exploits the spatial and temporal characteristics of the
 385 face image sequence is proposed for efficient matching. A simple deterministic
 386 algorithm to find similarity between the graphs is also proposed. Our future
 387 work will handle video sequences involving various pose of the faces, different
 388 resolutions, and video-to-video based recognition.

389 References

- 390 1. Chellappa, R., Wilson, C.L., Sirohey, S.: Human and machine recognition of faces:
 391 a survey. *Proceedings of the IEEE* **83** (1995) 705–741
- 392 2. Wang, H., Wang, Y., Cao, Y.: Video-based face recognition: A survey. *World*
 393 *Academy of Science, Engineering and Technology* **60** (2009)
- 394 3. Zhao, W., Chellappa, R., Phillips, P.J., Rosenfeld, A.: Face recognition: A literature
 395 survey (2000)
- 396 4. Turk, M., Pentland, A.: Eigenfaces for recognition. *Journal of Cognitive Neuro-*
 397 *science* **3** (1991) 71–86
- 398 5. Etemad, K., Chellappa, R.: Discriminant analysis for recognition of human face
 399 images. *Journal of the Optical Society of America* **14** (1997) 1724–1733
- 400 6. Moghaddam, B., Nastar, C., Pentland, A.: Bayesian face recognition using de-
 401 formable intensity surfaces. In *Proceedings of Computer Vision and Pattern Recog-*
 402 *nition* (1996) 638–645

- 403 7. Zhou, S., Krueger, V., Chellappa, R.: Probabilistic recognition of human faces
404 from video. *Computer Vision and Image Understanding* **91** (2003) 214–245
- 405 8. Manjunath, B.S., Chellappa, R., Malsburg, C.: A feature based approach to face
406 recognition (1992)
- 407 9. Ersi, E.F., Zelek, J.S.: Local feature matching for face recognition. In *Proceedings*
408 *of the 3rd Canadian Conference on Computer and Robot Vision* (2006)
- 409 10. Wiskott, L., Fellous, J.M., N.Kruger, Malsburg, C.V.D.: Face recognition by elastic
410 bunch graph matching. *IEEE Trans. on Pattern Analysis and Machine Intelligence*
411 **19** (1997) 775–779
- 412 11. Ersi, E.F., Zelek, J.S., Tsotsos, J.K.: Robust face recognition through local graph
413 matching. *Journal of Multimedia* (2007) 31–37
- 414 12. Zhou, S., Krueger, V., Chellappa, R.: Face recognition from video: A condensation
415 approach. In *Proc. of fifth IEEE International Conference on Automatic Face and*
416 *Gesture Recognition* (2002) 221–228
- 417 13. Li, Y.: *Dynamic face models: construction and applications*. Ph.D. Thesis, Uni-
418 *versity of London* (2001)
- 419 14. Kim, M., Kumar, S., Pavlovic, V., Rowley, H.A.: Face tracking and recognition
420 with visual constraints in real-world videos. *CVPR* (2008)
- 421 15. Stallkamp, J., Ekenel, H.K.: Video-based face recognition on real-world data (2007)
- 422 16. Liu, X., Chen, T.: Video-based face recognition using adaptive hidden markov
423 models. *CVPR* (2003)
- 424 17. Lee, K.C., Ho, J., Yang, M.H., Kriegman, D.: Visual tracking and recognition using
425 probabilistic appearance manifolds. *Computer Vision and Image Understanding*
426 **99** (2005) 303–331
- 427 18. Park, U., Jain, A.K.: (The 2nd international conference on biometrics, seoul,
428 korea, 2007 3d model-based face recognition in video)
- 429 19. Wu, Y., Roy-Chowdhury, A., Patel, K.: Integrating illumination, motion and shape
430 models for robust face recognition in video. *EURASIP Journal of Advances in*
431 *Signal Processing: Advanced Signal Processing and Pattern Recognition Methods*
432 *for Biometrics* (2008)
- 433 20. Ojala, T., Pietikainen, M., Harwood, D.: A comparative study of texture measures
434 with classification based on feature distributions. *Pattern Recognition* (1996) 51–59
- 435 21. Ojala, T., Pietikainen, M., Maenpaa, T.: A generalized local binary pattern opera-
436 tor for multiresolution gray scale and rotation invariant texture classification. *Sec-
437 ond International Conference on advances in Pattern Recognition, Rio de Janeiro,*
438 *Brazil* (2001) 397–406
- 439 22. Penev, P., Atick, J.: Local feature analysis: A general statistical theory for object
440 representation. *Network: Computation in Neural Systems* **7** (1996) 477–500
- 441 23. Mika, S., Rtsch, G., Weston, J., Schlkopf, B., Mller, K.R.: Fisher discriminant
442 analysis with kernels (1999)
- 443 24. McLachlam, J., Peel, D.: *Finite mixture models* (2000)
- 444 25. Redner, R.A., Walker, H.F.: Mixture densities, maximum likelihood and the em
445 algorithm. *SIAM Review* **26** (1984) 195–239
- 446 26. Lowe, D.G.: Distinctive image features from scale-invariant keypoints. *Internat-
447 ional Journal of Computer Vision* **60** (2004) 91–110
- 448 27. O’Toole, A., Harms, J., Hurst, S.L., Pappas, S.R., Abdi, H.: A video database of
449 moving faces and people. *IEEE Transactions on Pattern Analysis and Machine*
450 *Intelligence* **27** (2005) 812–816